Original article

Folia Neuropathologica

Non-woven nanofiber mats – a new perspective for experimental studies of the central nervous system?

Janina Rafalowska[1], Dorota Sulejczak[2], Stanisław J. Chrapusta[2], Roman Gadamski[1], Anna Taraszewska[1], Paweł Nakielski[3], Tomasz Kowalczyk[4], Dorota Dziewulska[1,5]

[1]Department of Experimental and Clinical Neuropathology, Mossakowski Medical Research Centre, Polish Academy of Sciences, Warsaw, [2]Department of Experimental Pharmacology, Mossakowski Medical Research Centre, Polish Academy of Sciences, Warsaw, [3]Department of Mechanics and Physics of Fluids, Institute of Fundamental Technological Research, Polish Academy of Sciences, Warsaw, [4]Department of Theory of Continuous Media, Institute of Fundamental Technological Research, Polish Academy of Sciences, Warsaw, [5]Department of Neurology, Medical University of Warsaw, Poland

Folia Neuropathol 2014; 52 (4): 407-416 DOI: 10.5114/fn.2014.47841

Abstract

(Sub)chronic local drug application is clearly superior to systemic administration, but may be associated with substantial obstacles, particularly regarding the applications to highly sensitive central nervous system (CNS) structures that are shielded from the outer environment by the blood-brain barrier. Violation of the integrity of the barrier and CNS tissues by a permanently implanted probe or cannula meant for prolonged administration of drugs into specific CNS structures can be a severe confounding factor because of the resulting inflammatory reactions. In this study, we tested the utility of a novel way for (sub)chronic local delivery of highly active (i.e., used in very low amounts) drugs to the rat spinal cord employing a non-woven nanofiber mat dressing. To this end, we compared the morphology and motoneuron ($\alpha + \gamma$) counts in spinal cord cervical and lumbar segments between rats with glutamate-loaded nanofiber mats applied to the lumbar enlargement and rats with analogical implants carrying no glutamate. Half of the rats with glutamate-loaded implants were given daily valproate treatment to test its potential for counteracting the detrimental effects of glutamate excess. The mats were prepared in-house by electrospinning of an emulsion made of a solution of the biocompatible and biodegradable poly(L-lactide-co-caprolactone) polymer in a mixture of organic solvents, an aqueous phase with or without monosodium glutamate, and sodium dodecyl sulfate as an emulsifier; the final glutamate content was 1.4 µg/mg of the mat. Three weeks after mat implantation there was no inflammation or considerable damage of the spinal cord motoneuron population in the rats with the subarachnoid dressing of a glutamate-free mat, whereas the spinal cords of the rats with glutamate-loaded nanofiber mats showed clear symptoms of excitotoxic damage and a substantial increase in dying/damaged motoneuron numbers in both segments studied. The rats given systemic valproate treatment showed significantly lower percentages of damaged/dying motoneurons in their lumbar enlargements. These results demonstrate the capacity of nanofiber mats for generation of neurotoxic glutamate in the rat CNS. However, the tested nanofiber mats need further improvements aimed at extending the period of effective drug release and rendering the release more steady.

Key words: *CNS injury, electrospinning, excitotoxicity, glutamate, motoneuron, nanofibers, neurodegeneration, spinal cord, valproate.*

Communicating author:

Dorota Sulejczak, Department of Experimental Pharmacology, Mossakowski Medical Research Centre, Polish Academy of Sciences, 5 Pawińskiego St., 02-106 Warsaw, Poland, phone: +48 22 608 65 23, fax: +48 22 668 65 27, e-mail: dsulejczak@imdik.pan.pl

Introduction

Targeted administration of active substances has clear advantages over systemic application. However, it may be associated with considerable obstacles in some cases, particularly regarding the chronic administration of drugs meant to affect specific central nervous system (CNS) structures that are shielded from the outer environment by the blood-brain barrier [10,13]. In most cases it is necessary to mechanically disturb the integrity of the meninges and the barrier. Such interventions additionally carry a risk of CNS tissues being damaged by the permanently implanted probe or cannula, which may be a severe confounding factor due to the consequential inflammatory reaction. This is why there is an ongoing search for alternative ways for delivering medicines to the CNS that lessen the risk of such complications [6,12,13,15].

In the case of drugs that are used in small (in mass and volume) quantities, an ideal solution would be to employ a carrier that: 1) is small enough to pose no problems at its implantation, and 2) degrades gradually to harmless metabolites over time, e.g., see [9], simultaneously releasing its active load at a rate necessary to create an effective concentration of the active principle. An effective solution of this problem may be in the use of nanomaterials, and particularly those made of electrospun fibers prepared from biocompatible/biodegradable polymers that have already been accepted for medical use.

Electrospinning is a process of forming nanofibers by interaction of a viscoelastic liquid stream (e.g., a polymer solution or melt, an emulsion, or other liquid-liquid systems) with a strong electric field. Such nanofibers have a thickness of several tens of nm to several μm and can be easily made into non-woven mats that can be used as drug carriers; for a review see [23].

The aim of this study was to test the utility of a novel way for (sub)chronic local delivery of active substances to the CNS with the use of such mats. To avoid instant discharge of the entire drug load and ensure long-term action of such a drug delivery system, the drug must be somehow enclosed within the nanofiber structural material. In the case of substances that cannot be dissolved in the latter, the nanofibers can be formed by emulsion electrospinning, with the drug being a component of the aqueous phase, or by coaxial electrospinning (core-shell system) [23]. A considerable potential for such applications is shown by nanofibers made of polycarbonates or aliphatic polyesters, which degrade *in vivo* relatively slowly (over many weeks, see [9]) by non-enzymatic random hydrolytic scission of esters linkage, to form small molecules identical to or homologous with endogenous metabolites or their analogs; the process is slow enough to cause no inflammation. Nanofibers made of these polymers can also aid appropriate healing of possible CNS trauma [1,24], which is likely due to their forming a temporary biocompatible scaffold for the cells taking part in this process [5].

To test the capacity of such material for effective delivery of an active substance *in vivo*, we chose mats carrying glutamate. As evidenced by many animal studies and clinical and post-mortem observations in humans, excessive glutamate accumulation in the interstitial space plays an important role in pathogenesis of many CNS disorders by causing injury and death of cells, and particularly of motoneurons, in both the brain and the spinal cord [14,22].

In the last decade, much attention was paid to the function of the excitatory amino acid receptors and their role in excitotoxicity, e.g., see [4,8,16,26]. Many of those experiments were performed with the use of microdialysis, which involves placement of the microdialysis probe (i.e., of a "foreign body") within the CNS, and the consequential nervous tissue damage and the emergence of (pro)inflammatory cytokines and other potentially harmful reactions. Establishing precisely the relationship between the effects of various noxious/pathogenic factors in such an experimental setup may be difficult or not feasible.

Neurotoxicity of exogenous and endogenous glutamate manifests itself, *inter alia*, in morphological changes occurring both in the cytoplasm and in the cell nucleus. Nuclear chromatin structure is mostly determined by the interaction of DNA with basic proteins – histones [21]. Increased histone deacetylase (HDAC) activity leads to condensation of the chromatin and silencing of gene expression, whereas inhibition of this activity causes rarefaction of chromatin and facilitates interaction between transcription factors and gene promoters, resulting in enhanced gene expression [7,28]. Perturbations of the acetylation/deacetylation balance can result in pathology and were found in various neurological disorders as well as in brain ischemia, in which HDAC inhibition usually plays an anti-inflammatory, neuroprotec-

tive and neurotrophic role [3,11,17,28]. Among many HDAC inhibitors, valproic acid [21] and its derivatives are widely used. Beside its utility in the treatment of bipolar disorders, epilepsy and migraine, it is also employed in a variety of acute CNS injuries [2]. Valproic acid was found to increase the expression of the survival motor neuron (SMN) protein in fibroblasts from patients with spinal muscular atrophy [25]. It also improves memory and inhibits neuritic plaque formation in a mouse model of Alzheimer disease [19]. Hence, in this study, we decided to test also the possibility of attenuating, with systemic valproate treatment, the pathomorphological changes evoked in the rat spinal cord by the glutamate released from the locally applied nanofiber mat.

Material and methods

Reagents for nanofiber mat production and analysis

Poly(L-lactide-*co*-caprolactone) Purasorb PLC 7015 (PLCL) containing 70% L-lactide and 30% caprolactone units was bought from Corbion Purac (Gorinchem, The Netherlands). Monosodium glutamate, *o*-phthalaldehyde and 2-mercaptoethanol were purchased from Sigma-Aldrich, and sodium dodecyl sulfate, chloroform, dimethylformamide, boric acid and sodium hydroxide were obtained from POCh S.A. (presently Avantor Performance Materials Poland S.A., Gliwice, Poland). All the chemicals were used without further purification.

Nanofiber mat preparation and characterization

Non-woven nanofiber mats were prepared by emulsion electrospinning, using a custom-made system as described elsewhere [18,23]. The emulsion was prepared as follows: 40 mg of sodium dodecyl sulfate was mixed with 1 g of 9% (w/w) solution of PLCL in a chloroform-dimethylformamide mixture (16 : 1, w/w). Fifty mg of 5% (w/w) monosodium glutamate solution in deionized water was added dropwise, with 30-s vortexing intervals, to the polymer/sodium dodecyl sulfate mixture. Next, the entire mixture was vortexed vigorously for 15 min in a tightly closed tube. Electrospinning was performed in a polycarbonate chamber of about 1 m^3 volume that shielded the working personnel from the high voltage employed and the final product from contamination with dust. The electrospinning setup was as follows: spinneret nozzle (made of 26G needle) to collector distance 15 cm, voltage 20 kV, and the emulsion flow of 0.2 ml/h. The forming nanofibers were collected on a rotating (1800 rpm) polypropylene cylinder (15 mm diameter) covered with grounded aluminum foil, to form a non-woven mat. The "empty" (glutamate-free) nanofiber mat was prepared by the same method except that the emulsion was devoid of glutamate. The mats were left on the collector for 24 h to release internal tension and avoid mat shrinkage, and then were removed from the collector together with the underlying aluminum foil and cut to the needed size with a fresh disposable surgical blade.

The morphology of the glutamate-loaded nanofiber mat was examined by scanning electron microscopy, using a model JSM 6390 LV microscope (Jeol, Japan). For the analysis, the mat was sputtered with gold using a model SC7620 Polaron mini sputter coater (Quorum Technologies Ltd., Ashford, UK). The analysis showed a network of partially adhering fibers of average diameter of 549 ± 206 nm (mean ± SD); see Fig. 1.

The capacity of the mat for gradual release of monosodium glutamate was evaluated *in vitro* as follows: a single sample of the mat (11 mg, about 11 mm × 11 mm) was placed in an Eppendorf tube with 1 ml of phosphate-buffered (10 mM, pH 7.4) 0.9% (w/v) solution of NaCl in deionized water (PBS), capped and incubated at 37°C. The incubation medium was sampled and replaced with fresh PBS at predetermined time intervals. The used medium

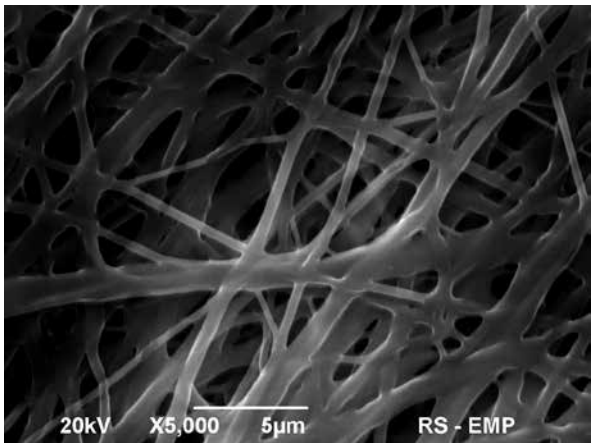

Fig. 1. Scanning electron microscope micrograph of the monosodium glutamate-containing PLCL nanofiber mat prepared by emulsion electrospinning.

samples were kept frozen at –20°C until analyzed. The concentration of glutamate in the samples was assessed after its conversion into a fluorescent derivative as described by Roth [20], with minor modifications. Briefly, the assay was performed in 96-well plates, using the reagent made by mixing 0.05 M borate buffer solution with ethanolic *o*-phthalaldehyde (10 mg/ml) and 2-mercaptoethanol solutions (5 µl/ml) 60 : 1 : 1 (v/v/v). Seventy-five µl aliquots (6 each) of fresh incubation medium (blank samples), used incubation medium samples and monosodium glutamate dilutions in PBS (standard samples) were pipetted into separate wells. Next, 75 µl of the borate buffer-mercaptoethanol-*o*-phthalaldehyde reagent mixture was added to each well and all samples were mixed immediately. Fluorescence intensity was measured within the next 5 min, using a model Fluoroskan Ascent spectrofluorimeter (Thermo Scientific, Rockford, IL, USA), with monochromators set at 355 nm (excitation) and 460 nm (emission measurement). The analysis (data not shown) revealed that the mat released about 0.8 µg of monosodium glutamate per mg of the mat during the first week; about 50% of this amount was released within the first few hours. After two weeks, the total amount released was 1.2 µg of the drug per mg of the mat (i.e., 8.4% of the initial content), and the estimated total amount released during 3 weeks (the planned duration of the *in vivo* rat experiment) was 1.7 µg per mg of the mat (12% of the initial content).

Animals and experimental design

Twelve adult male Wistar rats from the stock of the Mossakowski Medical Research Centre, Warsaw, Poland, initial body weight 250-300 g, were used for the study. The rats were housed three per opaque plastic cage (55 cm × 33 cm floor size) in an air-conditioned environment (21 ± 2°C, 60-70% relative humidity) under a 12 h light/12 h dark day cycle (lights on at 7 a.m.), with free access to standard laboratory rodent chow and tap water. The rats were randomly divided between four experimental groups: 1) intact rats (group I, $n = 3$); 2) rats subjected to surgical placement of a drug-free nanofiber mat into the spinal cord subarachnoid space at the lumbar level (group II, $n = 3$); 3) rats subjected to surgical placement of a monosodium glutamate-containing nanofiber mat into the spinal cord subarachnoid space at the lumbar level (group III, $n = 3$); and 4) rats subjected to surgical placement of a glutamate-loaded mat into the spinal cord subarachnoid space at the lumbar level and additionally given daily one dose of sodium valproate (Convulex syrup 50 mg/ml, Gerot Pharmazeutika, Vienna, Austria) by gavage (group IV, $n = 3$), beginning on the day of the surgery. The starting valproate dose was 33.3 mg/kg; the dosage was increased by 8.3 mg/kg each day for 4 consecutive days and then was kept constant for the rest of the study period.

The surgical procedure employed for submeningeal implantation of nanofiber mat pieces (approximately 5 mm × 5 mm size) into rat spinal cords (at the lumbar enlargement level) was as described elsewhere [1]. Three weeks after implantation of nanofiber mats, all rats were anesthetized with a lethal dose of sodium pentobarbital (80 mg/kg, i.p.) and decapitated. Spinal cords were excised and fixed in 4% formaldehyde in PBS and then embedded in paraffin using a standard procedure. All animal use procedures were in strict compliance with the European Union directive on the protection of laboratory animals (86/609/EEC) and with the current laws of Poland. All efforts were made to keep the number of rats used at a minimum and minimize animal discomfort. The experimental protocol has been accepted by the 4th Local Animal Experimentation Ethics Committee at the National Medicines Institute, Warsaw, Poland (Permit No. 43/210).

Histology and immunohistochemistry

The formalin-fixed and paraffin-embedded samples of rat spinal cords were cut transversely into 8 µm-thick sections. After deparaffinization and rehydration in a water-ethanol solution series, part of the sections were stained with violet cresyl using a routine procedure. Their sister slices were incubated with primary antibodies against synaptophysin (Dako Cytomation A/S, Denmark, cat. no. M0776; dilution 1 : 100), or GFAP (Dako cat. no. Z0334; dil. 1 : 2000), or neurofilament (Dako cat. no. M0762; dil. 1 : 100). Next, the samples were incubated with the respective secondary antibody (Beckman Coulter Inc., France, cat. no. IM0816, or IM0830; dil. 1 : 100) and then with streptavidin-horseradish peroxidase solution (Beckman Coulter cat. no. IM0309; dil. 1 : 500). The final immune complexes were visualized by a standard procedure employing diaminobenzidine as the chromogen, counterstained with hematoxylin, and assessed by light microscopy.

Ultrastructural studies

For electron microscopy studies, samples of lumbar spinal cord were taken and immediately fixed in a solution of 2% formaldehyde and 2.5% glutaraldehyde in cacodylate buffer pH 7.4 for 4 h, then they were divided into smaller pieces, rinsed in cacodylate buffer, postfixed in 1.0% OsO_4 for 1 h, dehydrated in a series of ethanol dilutions and embedded in Epon resin. Semi-thin sections stained with 1% toluidine blue were viewed in a light microscope for identification of motoneurons. Ultrathin sections were prepared from selected blocks, counterstained with uranyl acetate and lead citrate and then examined in a model JEOL 1200EX (Jeol, Japan) transmission electron microscope.

Assessment of the extent of damage to spinal cord motoneuron populations

Spinal cord samples used for motoneuron counting were taken from both the cervical enlargement (C4-C8 level) and the lumbar enlargement (L2-L6 level). The samples were fixed in 4% formaldehyde solution pH 7.4, dehydrated in a series of ethanol dilutions, embedded in paraffin, cut transversally into 8 µm thickness serial sections, and stained with cresyl violet using the routine procedure. Different sections from the same segment of the spinal cord can contain differing numbers of motoneurons. Therefore, three such sections from each of the two spinal cord segments of each rat, each section covering the whole of both ventral horns of the spinal cord, were used for quantitation. The sections were separated by at least 40 µm (along the spinal cord length) to avoid double counting of the same motoneurons. To facilitate the counting and avoid double counting the same cells, especially the relatively small γ-motoneurons, a 10 mm × 10 mm reticle with 20 divisions along each side was placed in the microscope eyepiece to overlap with the cross-section view of the spinal cord. The counting was performed in three "fields of observation" for each spinal horn (i.e., in six fields/section), and the counts from all six fields were added up for calculation of the percentage of damaged/dying motoneurons in a given rat and spinal cord segment.

Statistical analysis

Data on spinal cord motoneuron numbers were analyzed by repeated measures two-way ANOVA with group (I-IV) as the main factor and spinal cord segment (cervical enlargement and lumbar enlargement) as the repeated measures factor, followed by Fisher's least significant difference test. In all cases, $p < 0.05$ was considered significant.

Results

Spinal cord morphology and immunohistochemistry findings

Spinal cords of intact control rats showed normal morphology, with no detectable astrocytic reaction (Fig. 2). Morphological assessment revealed that implantation of nanofiber mats caused neither spinal cord damage nor inflammation in the rats with the subarachnoid dressing of an "empty" (glutamate-free) nanofiber mat (group II). The surface of their spinal cord motoneurons (both α and γ) showed a rosary-like arrangement of synapses; only a few of the cells showed symptoms of partial tigrolysis.

The rats with the subarachnoid dressing of a glutamate-carrying nanofiber mat (group III) revealed tigrolysis in a considerable fraction of their spinal cord motoneurons, including central tigrolysis in a number of the cells. In these rats, synaptophysin immunostaining showed substantial irregularities in the rosary-like arrangement of synapses on the surface of the cells, including loss of some synapses and only a residual thin band of reactivity in some cases. The astrocytic reaction was very weak, but hypertrophy and clasmatodendrosis were occasionally found. Spinal cord cross-sections also revealed distinct vasodilation, particularly of capillaries and venules, and the presence of subarachnoid hemorrhages as well as ecchymoses within the spinal cord (Fig. 2).

In group IV rats (with glutamate-loaded spinal cord dressing and systemic valproic acid treatment), the morphological changes in the ventral horns closely resembled those seen in the group III rats, except for a diminished number of tigrolytic cells (Fig. 2).

Results of neurofilament immunohistochemistry in rats from all experimental groups were very similar. The only difference was slightly stronger neurofilament immunoreactivity of the spinal cord gray matter due to increased density of immunoreactive neurofilament fibers and/or their more intense immunolabelling in group IV in comparison to group III (Fig. 2).

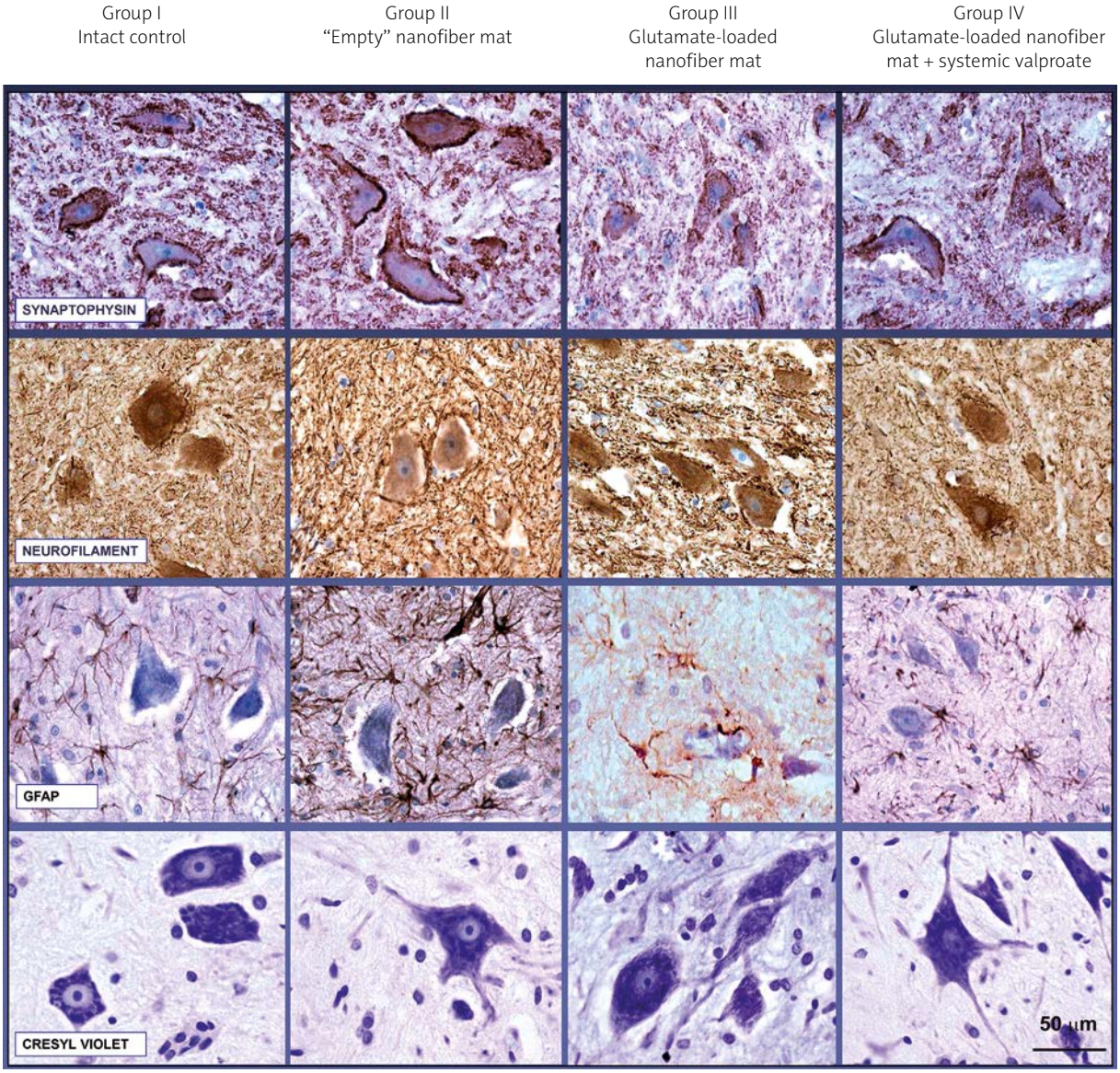

Fig. 2. Representative microphotographs illustrating the results of histological (cresyl violet staining) and immunohistochemical (synaptophysin, neurofilament and GFAP immunoreactivities) examination of spinal cords from all experimental rat groups.

Ultrastructural findings

In the control groups I and II, the motoneurons showed normal ultrastructure of their perikaryal cytoplasm with aggregates of long profiles of rough endoplasmic reticulum and the nucleus rich in hetero- and euchromatin (Fig. 3A). Mitochondria in the perikaryal cytoplasm, dendrites and axons were small and electron-dense. The neuropil showed the presence of numerous synaptic contacts on the neuronal somata and dendrites, and narrow spaces between cellular processes; see Fig. 3B.

In the group III rats, motoneuron perikaryal cytoplasm displayed depletion and dispersion of the rough endoplasmic reticulum (Fig. 3C), increased numbers of small vesicles and cisterns of the Golgi apparatus, and prominent swelling of the mitochondria (Fig. 3D); rarefaction of nuclear chromatin was evident as well. Dendrites were swollen and showed commonly the presence of numerous vesicles and disintegrated organelles; see Figs. 3C-D. Pathological changes (microvacuolization of cytoplasm and mitochondrial swelling) were also found in astrocytes and satellite

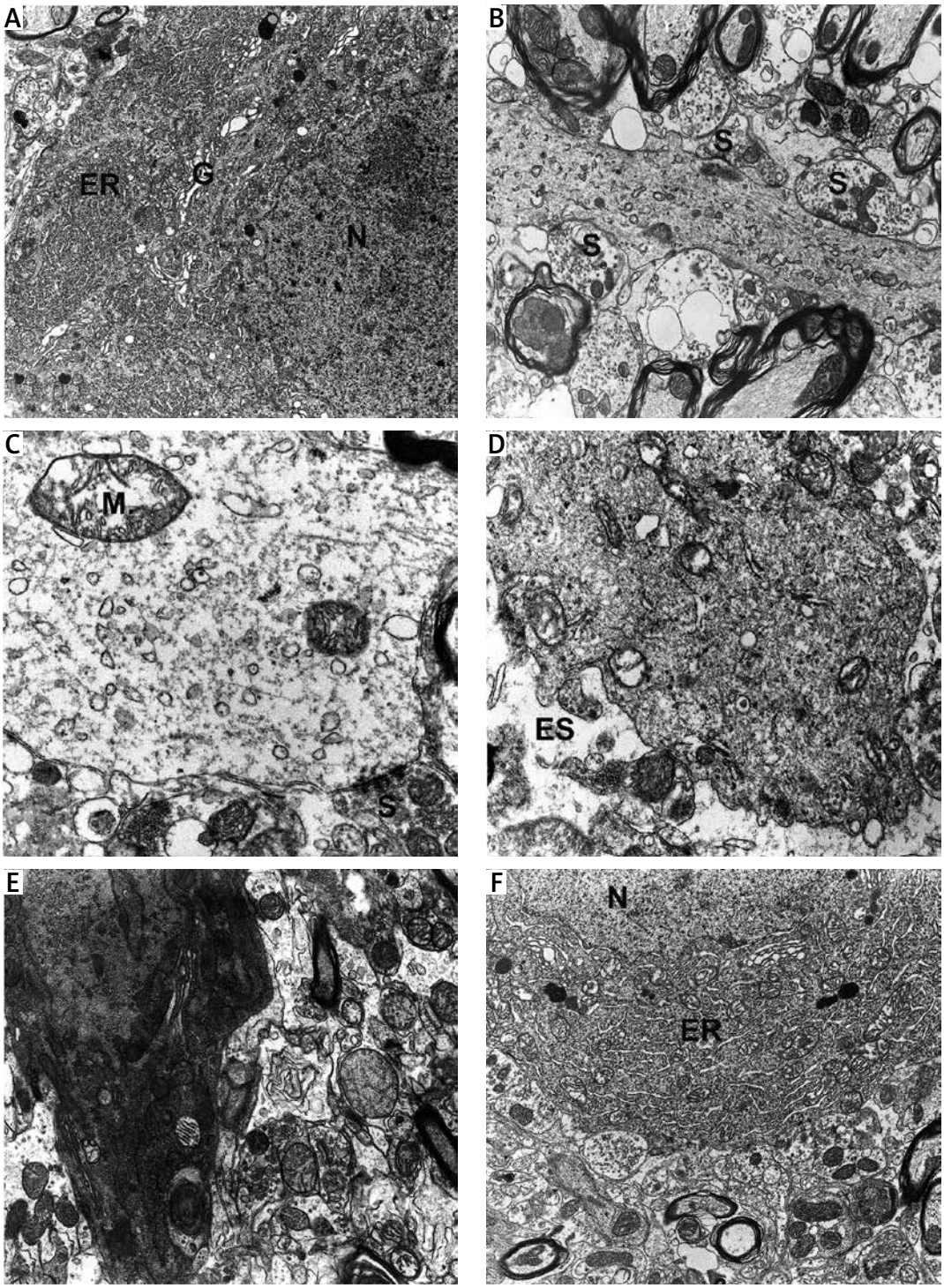

Fig. 3. Representative electronographs showing the ultrastructure of spinal cords from all experimental rat groups. **A-B)** Groups I and II. Note a well-preserved motoneuron cell body (in **A**) and a dendrite (in **B**). ER – endoplasmic reticulum, G – Golgi apparatus, N – nucleus, S – axo-dendritic synapse. Original magnification: × 3000 **(A)**; × 6000 **(B)**. **C-E)** Group III. Note swelling and microvacuolization of the dendrite cytoplasm (in **C** and **D**), and a "dark" motoneuron (in **E**). ES – enlarged extracellular space, M – swollen mitochondrium, S – axo-dendritic synapse. Original magnification: × 10 000 **(C, D)**; × 7500 **(E)**. **F)** Group IV. Motoneuron cell body with normal looking nuclear chromatin (N) and elongated profiles of rough endoplasmic reticulum (ER). Original magnification: × 5000.

oligodendrocytes, and in endothelial cells. The cellular changes were often associated with pericellular edema and loss of the axo-dendritic and axo-somatic synapses (Fig. 3E). Spinal cord motoneurons of group IV rats showed increased density of the nuclear chromatin and striking augmentation of the long profiles of rough endoplasmic reticulum in perikaryal cytoplasm (Fig. 3F).

Transmission electron microscopy also revealed partial degradation of the implanted mats (data not shown).

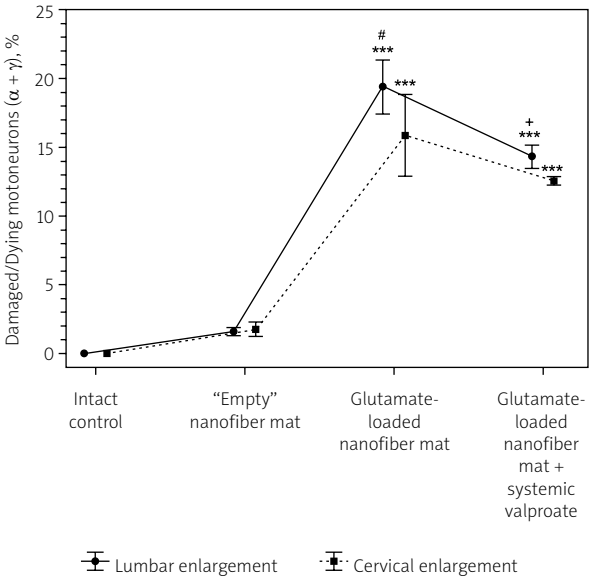

Fig. 4. Comparison of the damage to combined (α + γ) cervical and lumbar motoneuron populations in the various experimental groups. Note that the data for intact controls are shown only for illustration and were not included in statistical analyses. Repeated measures two-way ANOVA yielded a significant effect of both experimental group ($F_{2,6}$ = 410.6, $p < 10^{-3}$) and spinal cord region ($F_{1,6}$ = 8.74, p = 0.025) but no significant group × spinal cord region interaction on the combined percentages of damaged/dying motoneurons ($F_{2,6}$ = 3.39, p = 0.103). ***$p < 0.001$ vs. the respective value for the rats with implanted "empty" nanofiber mat, $^{\#}< 0.05$ vs. the respective value for the cervical enlargement of the same rats, $^{+}< 0.05$ vs. the respective value for the lumbar enlargement of the rats given no valproate.

Quantitative assessment of damage to spinal cord motoneuron population (see Fig. 4)

There was no difference between the experimental groups in the density of the combined motoneuron (α + γ) population in the studied spinal cord sections/segments (data not shown). No damaged/dying motoneurons were found in the ventral horns of control intact rats in either spinal cord segment studied. The rats with "empty" nanofiber mat application showed only a minute fraction of such cells, which was identical for the cervical and lumbar region. The rats given the spinal cord dressing of a glutamate-loaded nanofiber mat compared to both the intact rats and rats with the dressing of an "empty" nanofiber mat showed significant motoneuron damage in both these spinal cord segments; the damage was slightly but significantly greater in the lumbar region. The rats with an implanted glutamate-loaded nanofiber mat given systemic valproate treatment showed significantly but slightly lower percentages of damaged/dying motoneurons in their lumbar enlargements than their counterparts given no valproate, and a similar tendency (p = 0.062) was apparent for their cervical motoneurons.

Discussion

The toxicity of endogenous and exogenous glutamate is well established. In this study, we assessed the toxicity of exogenous glutamate to verify the idea of using, instead of probes permanently implanted into the CNS, which can cause major tissue damage, nanofiber mats as drug carriers. Importantly, probe implantation-related tissue damage can induce a variety of pathological phenomena that hinder the interpretation of experimental data.

We could not find, in the existing body of published scientific reports, any data on the use of nanofiber-based mats as drug carriers for chronic experiments. One of the questions to be answered was whether the amount of nanofiber mat that can be safely applied to the rat spinal cord using the laminectomy approach will be sufficient to provide an effective (as judged by a clear biological effect) drug dose. The subarachnoid space of the spinal cord is very narrow, which greatly limits the applicable size of the mat dressing. The use of smaller nanofiber mat fragments may necessitate a reduction of the mat-carried drug

dose, which may render it ineffective. Increasing drug concentration in the emulsion used for nanofiber mat production, with the aim of compensating the lessened size, may not be feasible because of some electrospinning-related physicochemical phenomena (e.g., those involving interactions of drug-derived ions; this was the case in this experiment, too). We were quite lucky in this regard because the amount of glutamate released during the 3-week *in vivo* study period, which represented but a minor fraction of the total drug contents of the implanted nanofiber mat pieces, exerted unambiguous toxic effects both in the spinal cord region adjacent to the location of the mat implant and in the more distant cervical segment of the spinal cord. The symptoms identified in the rats carrying glutamate-loaded nanofiber mat implants were typical of excitotoxic CNS insult (tigrolysis, postsynaptic dendrite swelling, clasmatodendrosis, and synaptic and neurofilament damage). Furthermore, numerous hemorrhages found in multiple locations of the spinal cord cross-sections and in the subarachnoid space clearly indicated blood-brain barrier damage, with thickening of small blood vessels possibly forecasting an increase in blood-brain barrier permeability. The absence of similar damage in the rats carrying "empty" nanofiber mat implants demonstrated that the PLCL mat itself was safe for the spinal cord and did not cause mere mechanical contact/size-related irritation either. The latter observation is in line with earlier studies performed in Mossakowski Medical Research Centre [1,24].

The beneficial effect of systemic valproate treatment on spinal cord motoneuron counts and morphology (decrease in the number of tigrolytic cells), as well as on synaptophysin immunoreactivity in the rats carrying glutamate-loaded nanofiber mat implants, suggested that the glutamate-induced damage was related to the effects of glutamate excess on histone acetylation/deacetylation. However, an alternative/additional explanation may be sought in the stimulatory effect of valproate on expression of the *SMN* gene [25]. Surprisingly, the valproate treatment did not improve blood-brain barrier impermeability, a finding that contrasts with the results of an earlier rat study [27]. This discrepancy was most likely related to the relatively low valproate dosage in our study and to its administration by gavage instead of the intraperitoneal route.

In summary, this study showed the potential of the tested nanofiber mat-based drug delivery system for (sub)chronic (a few weeks at least) administration of medicines to the CNS. The implanted nanofibrous carrier did not induce inflammatory changes either in the neighboring lumbar spinal cord region, or in the more distant cervical segment, or in the meninges, and underwent gradual biodegradation over time. As evidenced by the various approaches used for detecting glutamate-induced pathomorphological changes in our study, the tested PLCL nanofiber mat is suitable for generation of neurotoxic levels of excitatory amino acids in rat spinal cord as an alternative to mechanical probes that cause much more tissue damage. However, the tested nanofiber mat-based drug delivery system needs further improvements aimed at: 1) extending the period of effective drug release, 2) rendering the release more steady, and 3) eliminating the initial phase of 'burst' (of a few hours' duration) release of the carried drug.

Acknowledgments

This work was supported by grant no. NN 401 014640 from the Ministry of Science and Higher Education of Poland and by statutory funds from the Mossakowski Research Institute, Polish Academy of Science. The technical assistance of Tomasz Chmielewski and Aleksandra Kiszko of the Institute of Fundamental Technological Research, PAS, with preparation and *in vitro* characterization of the nanofiber mats is gratefully acknowledged.

Disclosure

Authors report no conflict of interest.

References

1. Andrychowski J, Frontczak-Baniewicz M, Sulejczak D, Kowalczyk T, Chmielewski T, Czernicki Z, Kowalewski TA. Nanofiber nets in prevention of cicatrization in spinal procedures. Experimental study. Folia Neuropathol 2013; 51: 147-157.
2. Chen S, Wu H, Klebe D, Hong Y, Zhang J. Valproic acid: a new candidate of therapeutic application for the acute central nervous system injuries. Neurochem Res 2014; 39: 1621-1633.
3. Chuang DM, Leng Y, Marinova Z, Kim HJ, Chiu CT. Multiple roles of HDAC inhibition in neurodegenerative conditions. Trends Neurosci 2009; 32: 591-601.
4. Corona JC, Tapia R. Ca^{2+}-permeable AMPA receptors and intracellular Ca^{2+} determine motoneuron vulnerability in rat spinal cord in vivo. Neuropharmacology 2007; 52: 1219-1228.
5. Delaine-Smith RM, Green NH, Matcher SJ, MacNeil S, Reilly GC. Monitoring fibrous scaffold guidance of three-dimensional collagen organisation using minimally-invasive second harmonic generation. PLoS One 2014; 9: e89761.

6. Gilmore JL, Yi X, Quan L, Kabanov AV. Novel nanomaterials for clinical neuroscience. J Neuroimmune Pharmacol 2008; 3: 83-94.
7. Hauser AT, Jung M, Jung M. Assays for histone deacetylases. Curr Top Med Chem 2009; 9: 227-234.
8. Hirata A, Nakamura R, Kwak S, Nagata N, Kamakura K. AMPA receptor-mediated slow neuronal death in the rat spinal cord induced by long-term blockade of glutamate transporters with THA. Brain Res 1997; 771: 37-44.
9. Jeong SI, Kim BS, Kang SW, Kwon JH, Lee YM, Kim SH, Kim YH. In vivo biocompatibilty and degradation behavior of elastic poly(L-lactide-co-ε-caprolactone) scaffolds. Biomaterials 2004; 25: 5939-5946.
10. Jiang X. Brain drug delivery systems. Pharm Res 2013; 30: 2427-2428.
11. Kazantsev AG, Thompson LM. Therapeutic application of histone deacetylase inhibitors for central nervous system disorders. Nat Rev Drug Discov 2008; 7: 854-868.
12. Kubinová S, Syková E. Nanotechnology for treatment of stroke and spinal cord injury. Nanomedicine (Lond) 2010; 5: 99-108.
13. Labuzek K, Gorki K, Jaroszek H, Jarzabek K, Gabryel B, Okopien B. Highly organized nanostructures for brain drug delivery – new hope or just a fad? CNS Neurol Disord Drug Targets 2013; 12: 1271-1285.
14. Leigh PN, Meldrum BS. Excitotoxicity in ALS. Neurology 1996; 47 (Suppl 4): S221-S227.
15. Liu T, Xu J, Chan BP, Chew SY. Sustained release of neurotrophin-3 and chondroitinase ABC from electrospun collagen nanofiber scaffold for spinal cord injury repair. J Biomed Mater Res A 2012; 100: 236-242.
16. Massieu L, Tapia R. Glutamate uptake impairment and neuronal damage in young and aged rats in vivo. J Neurochem 1997; 69: 1151-1160.
17. Meisel A, Harms C, Yildirim F, Bösel J, Kronenberg G, Harms U, Fink KB, Endres M. Inhibition of histone deacetylation protects wild-type but not gelsolin-deficient neurons from oxygen/glucose deprivation. J Neurochem 2006; 98: 1019-1031.
18. Nakielski P, Kowalczyk T, Zembrzycki K, Kowalewski TA. Experimental and numerical evaluation of drug release from nanofiber mats to brain tissue. J Biomed Mater Res B Appl Biomater 2014 May 13 [Epub ahead of print]. doi: 10.1002/jbm.b.33197.
19. Qing H, He G, Ly PT, Fox CJ, Staufenbiel M, Cai F, Zhang Z, Wei S, Sun X, Chen CH, Zhou W, Wang K, Song W. Valproic acid inhibits Aβ production, neuritic plaque formation, and behavioral deficits in Alzheimer's disease mouse models. J Exp Med 2008; 205: 2781-2789.
20. Roth M. Fluorescence reaction for amino acids. Anal Chem 1971; 43: 880-882.
21. Santini V, Gozzini A, Ferrari G. Histone deacetylase inhibitors: molecular and biological activity as a premise to clinical application. Curr Drug Metab 2007; 8: 383-393.
22. Shaw PJ, Eggett CJ. Molecular factors underlying selective vulnerability of motor neurons to neurodegeneration in amyotrophic lateral sclerosis. J Neurol 2000; 247 (Suppl 1): I17-I27.
23. Sill TJ, von Recum HA. Electrospinning: applications in drug delivery and tissue engineering. Biomaterials 2008; 29: 1989-2006.
24. Sulejczak D, Andrychowski J, Kowalczyk T, Nakielski P, Frontczak-Baniewicz M, Kowalewski T. Electrospun nanofiber mat as a protector against the consequences of brain injury. Folia Neuropathol 2014; 52: 56-69.
25. Sumner CJ, Huynh TN, Markowitz JA, Perhac JS, Hill B, Coovert DD, Schussler K, Chen X, Jarecki J, Burghes AH, Taylor JP, Fischbeck KH. Valproic acid increases SMN levels in spinal muscular atrophy patient cells. Ann Neurol 2003; 54: 647-654.
26. Wang Z, Leng Y, Tsai LK, Leeds P, Chuang DM. Valproic acid attenuates blood–brain barrier disruption in a rat model of transient focal cerebral ischemia: the roles of HDAC and MMP-9 inhibition. J Cereb Blood Flow Metabol 2011; 31: 52-57.
27. Yildirim F, Gertz K, Kronenberg G, Harms C, Fink KB, Meisel A, Endres M. Inhibition of histone deacetylation protects wildtype but not gelsolin-deficient mice from ischemic brain injury. Exp Neurol 2008; 210: 531-542.